

Sensor and Simulation Notes

Note 556

June 2011

Design, Realization and Experimental Test of a Coaxial Exponential Transmission Line Adaptor for a Half Impulse Radiating Antenna

Felix Vega

EMC Laboratory, Swiss Federal Institute of Technology of Lausanne (EPFL), Switzerland
Electrical and Electronic Engineering Department, National University of Colombia, Bogota, Colombia
felix.vega@epfl.ch

Farhad Rachidi

EMC Laboratory, Swiss Federal Institute of Technology of Lausanne (EPFL), Switzerland

Nicolas Mora

EMC Laboratory, Swiss Federal Institute of Technology of Lausanne (EPFL), Switzerland

Nestor Peña

Electrical and Electronic Engineering Department, Los Andes University, Bogota, Colombia

Francisco Roman

Electrical and Electronic Engineering Department, National University of Colombia, Bogota, Colombia

Abstract

This paper describes the simulation, design, realization and experimental test of a tapered transmission line for adapting a broadband impulse generator to a radiating antenna, for a frequency range of 50 MHz to 1 GHz. Two different taper geometries are considered and discussed in the analysis: exponential and logarithmic. Two analysis methods are also used: (1) analytical equations obtained by applying the transmission line theory, and (2) numerical simulations in both frequency- and time-domain using Comsol®. It is shown that in general an exponential taper performs better than a logarithmic one, especially at high frequencies. Time domain simulations reveals that for fast transient subnanosecond pulses, both tapers can be used equivalently and the signal does not suffer from any significant distortion while traveling along the tapers. We also show that analytical equations obtained using the transmission line theory are in very good agreement with full-wave simulation results and can be used advantageously in the design of tapers. The paper also presents the mechanical design and the realization of an exponential taper used for the connection of a 50- Ω pulser to a Half Impulse Radiating Antenna (HIRA) having an input impedance $Z_A = 100 \Omega$. The realized taper is fully characterized in frequency-domain using a vector analyzer and in time domain using a reflectometer and shown to be performing in agreement with the simulations.

I. INTRODUCTION

Matching of impedances to transmission lines is of capital importance to ensure signal integrity [1].

In the case of a single-frequency or narrow band signals, diverse matching networks, consisting of lumped elements or transmission line segments, can be successfully implemented (e.g. [2])

The situation is quite different when impedance matching is required over a wide band of frequencies. In this case, matching can be achieved by using a tapered transmission line.

The aim of the present study is the matching of a $50\ \Omega$ impulse generator to a Half Impulse Radiating Antenna (HIRA) having an input impedance $Z_A = 100\ \Omega$. The impulse voltage contains energy in a band of frequencies ranging from DC to about 1 GHz. Achieving good matching at low frequencies requires the use of a long tapered transmission line [3] which is impractical for this type of applications. We decided therefore to work in a band of frequencies between 50 MHz and 1 GHz, which coincides with the bandwidth of the considered HIRA.

The HIRA consists of a half parabolic reflector placed over a ground plane [4]. The reflector is illuminated by two TEM Horn feeders connected to an impulse voltage source. The feeders are connected to the reflector through a set of matching resistors. A description of the ensemble can be seen in Fig 1. The HIRA is a modified monopolar version of the Full IRA, presented by Baum in [5]. Both devices have been used to produce impulse electromagnetic fields in several applications, such as EMC immunity testing and ground penetrating radar (e.g. [6]). The main advantage of using a HIRA, instead of a Full IRA, is that it avoids the use of high voltage baluns, permitting the use of unbalanced sources, for example coaxial generators.

This paper is organized as follows. In Section II a brief description of the theory of tapered transmission lines is presented. Section III presents the design of an exponential tapered coaxial transmission line, as well as the theoretical analysis and the simulation of the response of the proposed design. The design of a logarithmic tapered coaxial transmission line is presented in Section IV, and a comparison between exponential and logarithmic tapers is presented in Section V. In Section VI we describe the manufacturing process of the taper. Section VII presents the measurements of the impedance of the taper along its length using a time domain reflectometer. Section VIII presents the characterization of the taper in time domain. Section VIII presents measurements results of the characterization of the taper in frequency domain. Conclusions are presented in Section IX.

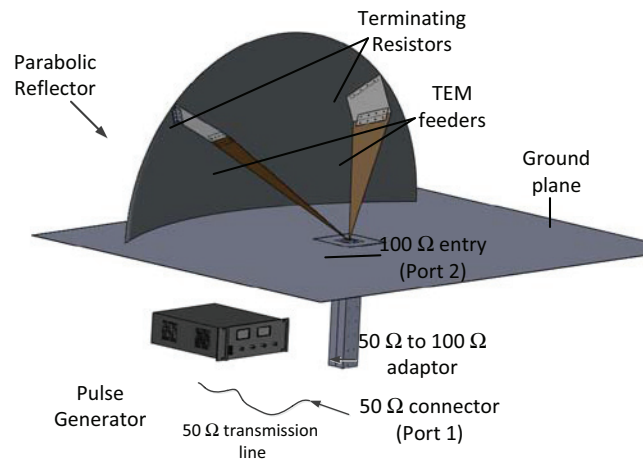


Fig 1 Half Impulse Radiating Antenna (HIRA), electronic pulse generator and taper adaptor

II. TAPERED TRANSMISSION LINES

Tapered transmission lines have been used as high pass matching devices, for both, harmonic and transient signals. When discussing frequency domain applications, the work presented by Collin [7] constitutes the reference for exponentially varying tapered transmission lines. In [8], Klopfenstein proposes an optimum tapered adaptor that presents a minimum reflection coefficient at its input for a determined transmission line length.

Propagation of short pulses along tapered transmission lines has been investigated for applications ranging from laser driving circuits [9-12] to matching of UWB circuits and antennas [13, 14].

In [3], Baum and Lehr analyzed the use of tapered transmission line transformers for high voltage pulses, concluding that the exponential profile minimizes the pulse droop after the initial rise time.

In [15], the construction of a logarithmic varying coaxial adaptor for HIRAs is presented.

A preliminary remark on the used terminology to describe the tapered lines is in order. In this paper, the terms ‘exponential’ and ‘logarithmic’ refer to the profile of the impedance, rather than the geometrical profile of the line along its length.

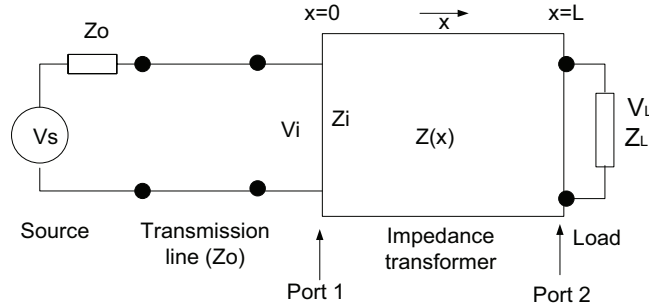


Fig 2 Circuit diagram of the Impedance adaptor

III. EXPONENTIALLY TAPERED TRANSMISSION LINE

A general circuit diagram of a tapered transmission line (TL) for matching a source to a load is presented in Fig 2 in which the tapered line is represented by a two-port circuit. The characteristic impedance of the matching line $Z(x)$ should vary smoothly as a function of the distance x , from the impedance of the source Z_0 at Port 1, $x=0$, to the impedance of the load Z_L at Port 2, $x=L$.

The quality of the matching in the frequency domain can be expressed in terms of the reflection coefficient at Port 1 $\Gamma(f)$:

$$\Gamma(f) = \frac{Z_i(f) - Z_0}{Z_i(f) + Z_0} \quad (1)$$

where Z_i is the input impedance of the matching TL.

$\Gamma(f)$ depends on the length of the matching TL L , the variation of the impedance as a function of x and the frequency of operation f . It can be evaluated [7] by solving the differential equation:

$$\frac{d\Gamma(f)}{dx} = \Gamma(f)2j\beta - \frac{1}{2}(1 - \Gamma(f)^2) \frac{\partial}{\partial x} \left(\ln \left(\frac{Z(x)}{Z_0} \right) \right) \quad (2)$$

$$\beta = \frac{2\pi f}{v_p} = \frac{2\pi f \sqrt{\epsilon_r}}{c} \quad (3)$$

in which v_p is the wave propagation speed, c is the speed of light and ϵ_r is the relative permittivity of the dielectric filling material.

If $Z(x)$ is assumed to vary exponentially,

$$\begin{aligned} Z(x) &= Z_0 e^{ax} \\ 0 &\leq x \leq L \end{aligned} \quad (4)$$

an analytical solution for Equation(2) can be derived [7]

$$\Gamma(f) = \frac{C \sin\left(\frac{RL}{2}\right)}{R \cos\left(\frac{RL}{2}\right) + 2j\beta \sin\left(\frac{RL}{2}\right)} \quad (5)$$

The exponential factor a in (4) can be determined as a function of the source and load impedances:

$$a = \frac{1}{L} \ln \left(\frac{Z_L}{Z_0} \right) \quad (6)$$

And the factors C , and R in (5) are given by:

$$C = \ln \left(\frac{Z_L}{Z_0} \right) \frac{1}{L} \quad (7)$$

$$R = \sqrt{4\beta^2 - C^2} \quad (8)$$

when $\beta \gg C/2$ Equation (8) reduces to:

$$R \cong 2\beta \quad (9)$$

And Equation (5) reduces to:

$$\Gamma(f) \cong \frac{1}{2} e^{-j\beta L} \ln \left(\frac{Z_L}{Z_0} \right) \frac{\sin(\beta L)}{\beta L} \quad (10)$$

This is a high frequency approximation; however, in our case the difference between equation (10) and (5) at low frequencies is negligible.

The zeros of Equation (10) are located at frequencies:

$$\frac{2\pi f_0 L}{v_p} = \pi, 2\pi, \dots, n\pi \quad (11)$$

$$f_0 = \frac{v_p}{2L}, \frac{v_p}{L}, \dots, \frac{nv_p}{2L}$$

where n is positive integer.

From Equation (10) it can be deduced that $\Gamma(f)$ depends on the ratio $(L\sqrt{\epsilon_r})/\lambda$. The bigger this factor, the faster the decrease of Γ as a function of frequency.

However, due to space restrictions related to the size of the HIRA, the line should not be larger than 0.7 m. Therefore in order to increase the electric length of the line, a dielectric filling material with $\epsilon_r = 2.2$ was chosen.

Replacing these values in Equation (5) and taking into account that the required minimum matching frequency is 50 MHz, the calculated physical and electrical lengths of the line to ensure a reflection coefficient $\Gamma(f) < -10$ dB are given by:

$$L = 0.6(m) \quad (12)$$

$$L_e = \sqrt{\epsilon_r} L = 0.88(m)$$

where L_e is the equivalent electric length of the line.

Fig 3 shows $\Gamma(f)$ as a function of the frequency. It can be seen that the matching criterion $\Gamma(f) < -10$ dB is fulfilled for frequencies above 50 MHz

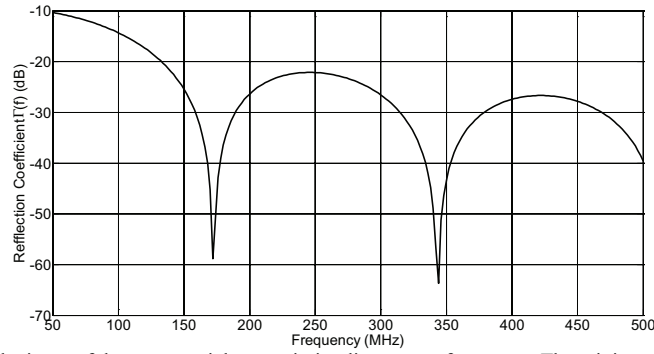


Fig 3. Reflection coefficient at the input of the exponential transmission line versus frequency. The minimum matching frequency is 50 MHz.

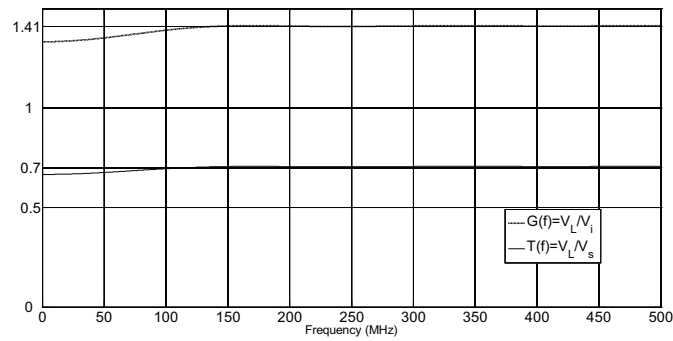


Fig 4. Magnitude of the voltage transfer functions in frequency domain.

The transfer function T between $V_L(f)$ and $V_S(f)$ can be evaluated as [9]:

$$T(f) = \frac{V_L}{V_S} = \sqrt{\frac{Z_L}{Z_o}} \frac{k_1 e^{-jk_2 L}}{(1+k_1) + e^{-2jk_2 L} (-1+k_1)} \quad (13)$$

where:

$$k_1 = \sqrt{1 - \frac{a^2}{4\beta^2}} \quad (14)$$

$$k_2 = \sqrt{\beta^2 - \frac{a^2}{4}} \quad (15)$$

The voltage “amplification factor” $G(f)$ of the taper can be defined as:

$$G(f) = \frac{V_L}{V_i} = 2T(f) \quad (16)$$

The factor $G(f)$ can be thought of as the ratio of the voltage effectively delivered to the load ($Z_L=100 \Omega$) and the voltage that would have been delivered in the absence of the taper and for a matched load ($Z_L=50 \Omega$).

Fig 4 shows both $T(f)$ and $G(f)$ as a function of frequency. It can be seen that at high frequencies, $V_L(f)$ is 70% of $V_S(f)$. At the same frequency range, it can be seen that $V_L(f)$ is 1.4 times as large as $V_i(f)$.

A. Taper Geometry Design

The tapered transmission line performs a physical transition between the output connector of the generator (Coaxial N, chassis-mount connector), and the antenna's input connector.

At the input port, the sizes of the inner (r_1) and outer (r_2) conductors of the taper should correspond to the N-type chassis-mount connectors, namely:

$$r_1(0)=1.5 \text{ mm}, r_2(0)=5.2 \text{ mm} \quad (17)$$

At the output port, the taper is connected to the coaxial input port of the antenna, with radii:

$$r_1(L)=2.5 \text{ mm}, r_2(L)=30 \text{ mm} \quad (18)$$

It can be seen that the radius of the inner conductor must vary from 1.5 mm to 2.5 mm over a length of 600mm, following some progressive profile. The simplest assumption is a linear variation between these two values. Manufacturing such a geometry in a CNC machine or in a lathe is quite a challenge. In order to avoid that, the whole taper was divided in three regions, the profile of which is illustrated in Fig 5.

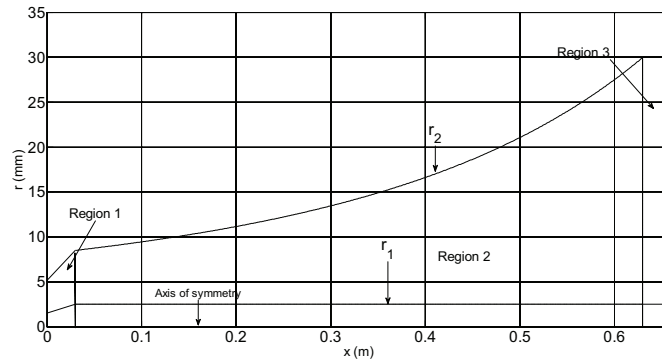


Fig 5 Profile of the taper as a function of the longitudinal distance (x and r axes are not in the same scale)

In region 1, we have a 30-mm long, 50Ω coaxial conical transmission line. In this section, both the inner and the outer conductors increase linearly with the longitudinal distance.

In region 2, we have a coaxial transition, with an impedance varying exponentially from 50Ω to 100Ω , over a total length of 600 mm.

Finally, in region 3, we have a 30-mm long, 100Ω coaxial cylindrical transmission line.

The overall length of the taper is 660 mm. The geometrical details of the 3 regions are summarized in Table 1.

TABLE 1 GEOMETRICAL AND ELECTRICAL PARAMETERS OF THE EXPONENTIAL TAPER'S THREE SECTIONS.

	Section 1		Section 2		Section 3	
Type	Co-Conical		Exponential		Coaxial	
x	$x=0$	$x=30$	$x=30$	$x=630$	$x=630$	$x=660$
r_1	1.5	2.5	2.5	2.5	2.5	2.5
r_2	5.2	8.5	8.5	30	30	30
$Z(x)$	50Ω	50Ω	50Ω	100Ω	100Ω	100Ω

Along the exponential section of the line (region 2), the characteristic impedance is given by:

$$Z(x) = \frac{60}{\sqrt{\epsilon_r}} \ln \left(\frac{r_2(x)}{r_1(x)} \right) (\Omega) \quad (19)$$

where $r_1(x)$ is constant and given by:

$$r_1(x) = 2.5 \text{ (mm)} \quad (20)$$

Using Equations (20) and (21), an exponential profile for the impedance can be achieved by calculating $r_2(x)$ as:

$$r_2(x) = r_1(x) \exp\left(\frac{50\sqrt{\epsilon_r}}{60\sqrt{\epsilon_r}} e^{a(x-0.03)}\right) (mm) \quad (21)$$

$$30 \text{ (mm)} < x < 630 \text{ (mm)}$$

in which a is given by(6).

A plot of the variation of the taper impedance as a function of the longitudinal distance x is shown in Fig. 6.

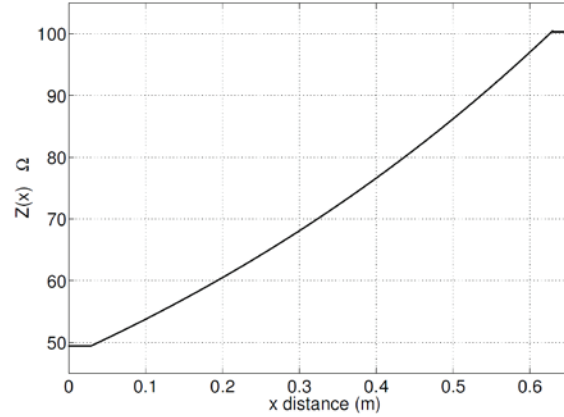


Fig 6 The impedance of the tapered transmission line along the longitudinal distance

B. Numerical Simulations

Frequency Domain Simulations

The designed taper was simulated in the frequency domain using the 2D-axial symmetry, frequency-domain TM-wave module in Comsol®.

The geometry used in the simulation is presented in Fig 7. It consists of a 2-D cut of the taper line. In order to compare the results with the analytical solution (10), we have considered a purely exponential profile along the taper. The inner and outer conductors are modeled as perfect electric conductors (PEC). The central axis of the coaxial is the rotational symmetry axis of the geometry. A signal, 1 W in power was applied to Port 1 (50 Ω). At the output port (Port 2) a 100 Ω coaxial port was defined. The frequency range of the signal is 50 MHz to 500 MHz.

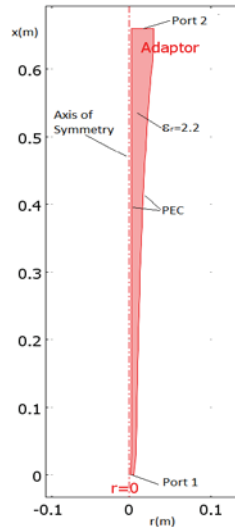


Fig 72-D geometry simulation setup. The profile defined in Fig 5 was imported in Comsol®.

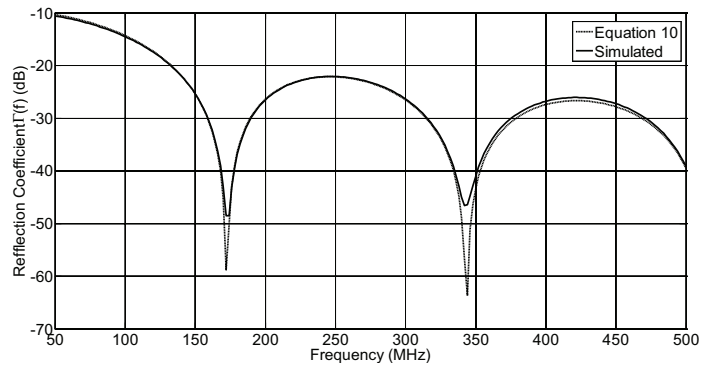


Fig 8 $\Gamma(f)$, Simulated using Comsol® and analytical, calculated using Equation (10)

Fig 8 depicts simulated results for $\Gamma(f)$, along with the theoretical results obtained using Equation (10). It can be seen that the analytical solution (10) yields results in very good agreement with numerical simulations.

Fig 9 presents simulated values of S_{21} as a function of frequency. Note that at high frequencies, the obtained values for S_{21} are very close to 0 dB, meaning that all the energy coupled to Port 1 reaches Port 2

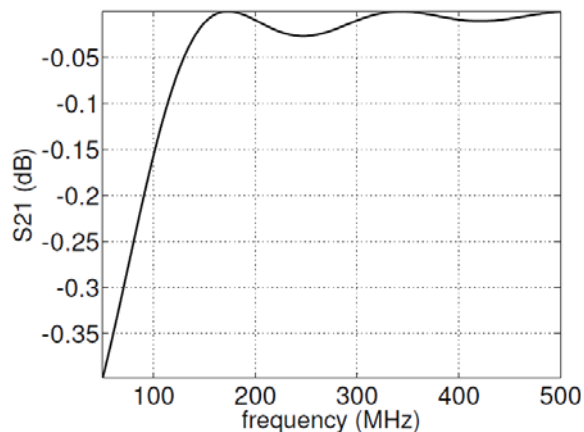


Fig 9 S_{21} (dB) obtained by simulation

The magnitude of the simulated and analytical transfer functions are shown in Fig 10. The simulated $T(f)$ was calculated using the scattering parameters produced by the simulation as follows [16]:

$$|T(f)| = \left| \frac{V_L(f)}{V_s(f)} \right| = \left| \sqrt{\frac{Z_L}{Z_0}} \frac{S_{21}(f)}{2} \right| \quad (22)$$

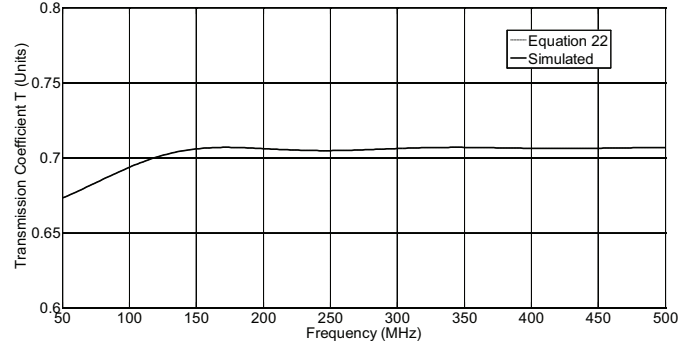


Fig 10 Transfer function $T(f)$ obtained by numerical simulations and using Equation (23). Both results are nearly identical.

Time Domain Simulations

In order to analyze the distortion and attenuation of the applied signal while traveling through the taper, time domain simulations were carried out.

The taper was simulated using the time-domain 2D-axial symmetry, TM-wave, module in Comsol®. The geometry is the same illustrated in Fig 7.

A voltage source producing a double exponential pulse $V_s(t)$ was connected to Port 1. The output impedance of the source was set to 50Ω . Port 2 is terminated on a coaxial impedance of 100Ω .

The signal of the source was defined as:

$$V_s(t) = V_p \left(e^{-\alpha t} - e^{-\beta t} \right) \quad (23)$$

with

$$\begin{aligned} \alpha &= 3e8 \text{ s}^{-1}, \\ \beta &= 1e9 \text{ s}^{-1}, \\ V_p &= 2.42 \text{ V} \end{aligned}$$

The rise time and decay time of $V_s(t)$ correspond to the waveform of the pulser which will be applied to the HIRA, namely rise time = 900 ps, FWHM = 4.7 ns.

The signals at the source $V_s(t)$, at the input port $V_i(t)$, and at the load $V_L(t)$ are shown in Fig 11. Note that the rise time of the output pulse is preserved.

The amplitude of $V_L(t)$ is 70% of that of $V_s(t)$, therefore an “amplification” factor $G = 1.4$ can be inferred, in agreement with Equation (17).

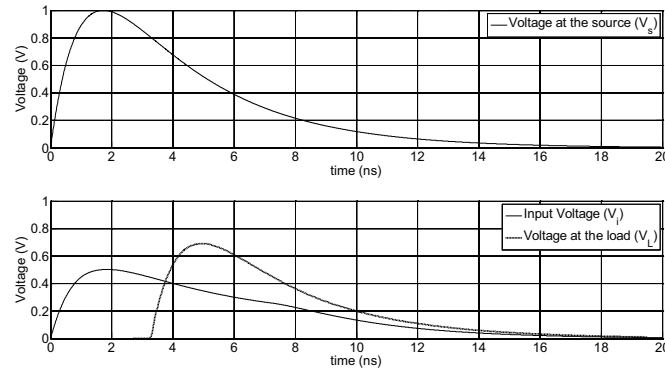


Fig 11 Time-domain simulation results. Voltages at the source, input and load. Note that the rise time of the signal at the load is preserved

IV. LOGARITHMIC COAXIAL TAPER

In this Section, we will compare the performance of the exponential taper with that of a coaxial logarithmic taper of the same electric length.

A. Taper Geometry Design

The logarithmic taper is generated by varying linearly the radius of the conductors. The logarithmic taper is again divided in three regions similar to the exponential taper (see the profile in Fig 12).

The inner conductor of the logarithmic taper is identical to the inner conductor of the exponential taper. The overall geometrical and electrical parameters are summarized in Table 2.

TABLE 2 GEOMETRICAL AND ELECTRICAL PARAMETERS OF THE LOGARITHMIC TAPER'S THREE SECTIONS.

	Section 1		Section 2		Section 3	
Type	Co-Conical		Linear		Coaxial	
x	$x=0$	$x=30$	$x=30$	$x=630$	$x=630$	$x=660$
r_1	1.5	2.5	2.5	2.5	2.5	2.5
r_2	5.2	8.5	8.5	30	30	30
$Z(x)$	50Ω	50Ω	50Ω	100Ω	100Ω	100Ω

In region 2, the outer conductor of the logarithmic taper is described by the linear equation:

$$r_2(x) = (7.4 + 3.58x)(mm) \quad (24)$$

$$30 \text{ mm} \leq x \leq 630 \text{ mm}$$

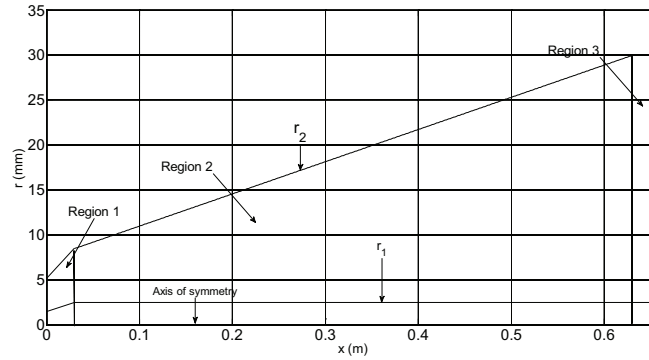


Fig 12 Profile of the logarithmic taper, as a function of the longitudinal distance (x and r axes are not in the same scale)

The logarithmic impedance of the taper along the linear region 2 is given by

$$Z(x) = \frac{60}{\sqrt{\epsilon_r}} \ln \left(\frac{r_2(x)}{r_1(x)} \right) = \frac{60}{\sqrt{\epsilon_r}} \ln \left(\frac{7.4e-3 + 0.0358x}{2.5e-3} \right) \quad (25)$$

Fig 13 presents the variation of the impedance as a function of the axial coordinate along the taper.

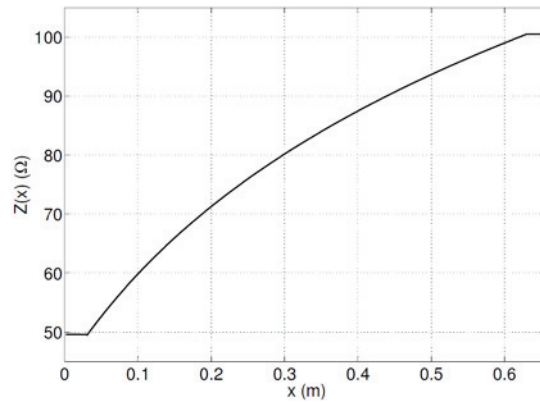


Fig 13. Impedance of the logarithmic tapered transmission line along the longitudinal distance.

Frequency Domain Analysis

The reflection coefficient can be obtained by inserting (26) in (2) and solving the resulting differential equation. Collin [7] simplified Equation (26) by neglecting the re-reflections in the line, leading to Equation (27), that was solved numerically using Mathematica®:

$$\begin{aligned} \Gamma(\theta) &= \frac{1}{2} \int_{L_1}^{L_2} e^{(-2j\beta x)} \frac{d}{dx} \left(\ln \left(\frac{Z(x)}{Z_0} \right) \right) dx \\ &= \frac{1}{2} \int_{L_1}^{L_2} e^{(-2j\beta x)} \frac{d}{dx} \ln \left(\ln \left(\frac{60}{Z_0 \sqrt{\epsilon_r}} \ln \left(\frac{7.4e-3 + 0.0358x}{2.5e-3} \right) \right) \right) dx \end{aligned} \quad (26)$$

The magnitudes of the reflection coefficient of the logarithmic and exponential tapers are presented in Fig 14. Note that the minimum matching frequency coincides in both cases. However, in the exponential case the reflection coefficient decreases faster with frequency, indicating a better matching as the frequency increases.

Time Domain Simulations

The logarithmic taper was simulated in time domain using the 2D axial symmetry, TM wave module in Comsol®. The simulation setup is equivalent to the one described in Section III.B. Again, we have considered here a pure logarithmic taper, i.e. Regions 1 and 2 were not included

The input and output signals are shown in Fig 15. It can be seen that, as for the exponential taper, the impulse voltage is not distorted while traveling through the logarithmic taper. The amplitude of the output impulse is again 70% of that of the impulse at the source, therefore a gain factor $G=1.4$ can be inferred.

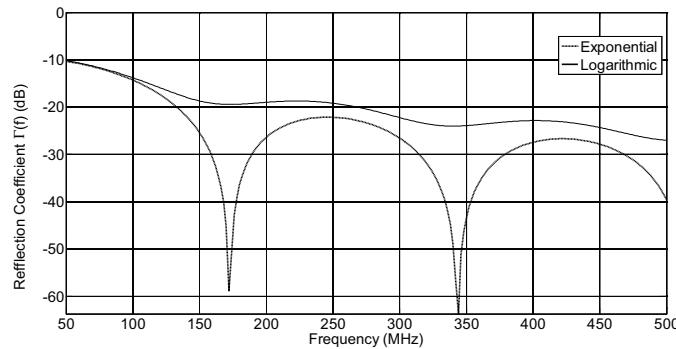


Fig 14 Magnitude of $\Gamma(f)$ at the entrance of the logarithmic and exponential tapers. Note that the matching frequency in both cases is 50 MHz, however $\Gamma(f)$ decays faster for the exponential taper.

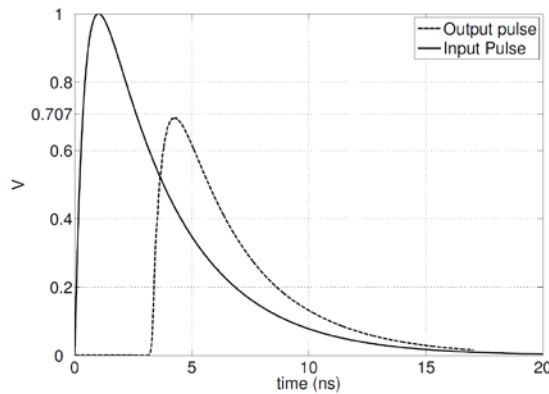


Fig 15 Signal at the source and signal at the load for a logarithmic taper. The rise time of the output pulse is preserved.

V. EXPONENTIAL TAPER VS. LOGARITHMIC TAPER

Question arises on whether to use an exponential or a logarithmic taper.

We have seen (Fig 14) that in the frequency domain, the two tapered lines behave similarly at low frequencies (<100 MHz). At higher frequencies, the exponential taper outperforms the logarithmic taper. In time domain, for the considered impulse characterized by a 800-ps risetime, both tapers result virtually in the same output impulse.

Therefore, we can conclude that for this specific application the results of both tapers are nearly identical. However, in a different scenario, the exponential taper can be more convenient; for example if a faster signal, with most of its spectral content located in high frequencies is applied, the exponential taper will produce less distortion to the signal.

Another point to consider is that the HIRA can be used for radiation of sinusoidal signals as well. In that case, for frequencies exceeding 100 MHz, the exponential taper would be definitely a better choice.

Regarding the mechanical construction of the tapered line, the logarithmic taper appears to be easier to fabricate, for example using a lathe. However, producing a conical profile over such a length, using a lathe is not a plausible alternative. Carving the line's profile would require the use of a CNC machine, as it will be described in Section VI. In this case carving either an exponential or a linear profile represents the same challenge.

In conclusion, the exponential taper has a better performance in frequency and its construction does not represent any extra effort compared to a logarithmic taper. In the next section, we will present the design and construction of an exponential taper only.

VI. MECHANICAL DESIGN AND CONSTRUCTION OF THE EXPONENTIAL TAPER

The taper is composed of three parts: the outer conductor, the inner conductor and the dielectric.

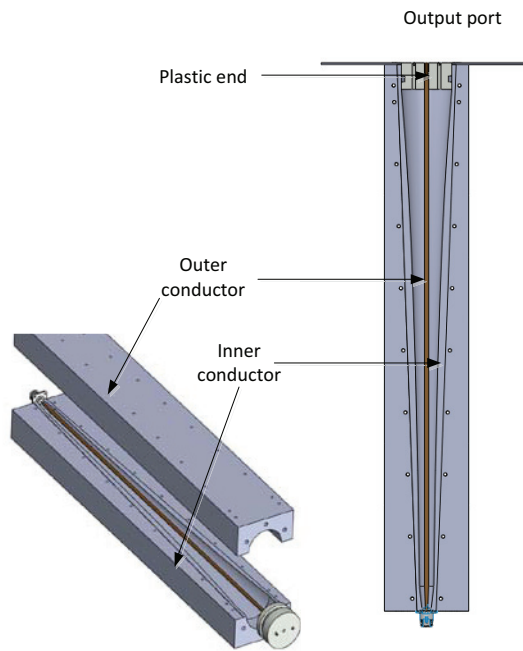
The inner conductor is formed by a copper conductor, lathed according to the 3-section profile (see Table 1)

The outer conductor was fabricated in aluminum using a CNC machine. Due to mechanical constraints, the conductor could not be manufactured from a single solid piece. The CNC machine cannot indeed carve into the metal on the axial direction x , over the total length of 0.66 m. Instead of that, the external conductor was split longitudinally in two halves and each half was carved tangentially according to the defined profiles for each one of the three sections of the taper.

The dielectric filling material selected for this taper is mineral oil used in transformers ($\epsilon_r=2.2$). The oil fills regions 1 and 2. In region 3, a plastic cap made of high density polyethylene was inserted in order to contain the oil inside the cavity. The plastic cap has nearly the same dielectric constant (2.2), assuring therefore the impedance continuity.

A 3-D view and a cut view of the CAD model generated in Solidworks® is shown in Fig 16

A photograph of the machined metallic halves is shown in Fig 17.



N Connector

Fig 16 Cut view (right) and 3-D exploded view (left-bottom) of the exponential taper



Fig 17 Pieces forming the coaxial taper

VII. TIME DOMAIN MEASUREMENTS

The taper was assembled, tightened and filled with mineral oil. No leaks were detected between the pieces.

The time domain response was measured using a Tecktronix® SD-24 Time Domain Reflectometer (TDR).

The TDR was connected to Port 1 (input of the taper) and Port 2 (taper output) was short circuited. The propagation velocity of the wave in oil (66% of the wave's velocity in vacuum) was taken into account in the configuration of the TDR.

The measurement of the impedance as a function of distance is presented in Fig 18, and compared with the theoretical values predicted by Equation (20).

It can be seen that, besides the observed limited effects of the 50 Ohm connectors, there is an excellent agreement between measured and theoretical responses. It can also be concluded from this figure, that neither dispersion nor tangent losses are detectable in the filling oil.

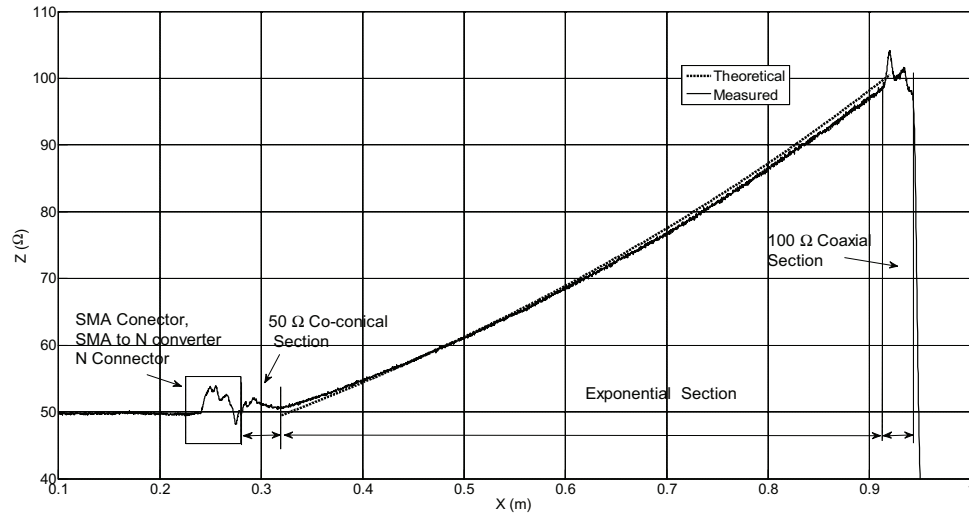


Fig 19 Impedance variation of the taper adaptor filled with oil, TDR measurement (solid line), theoretical (dashed line). Notice the correspondence between the two graphics.

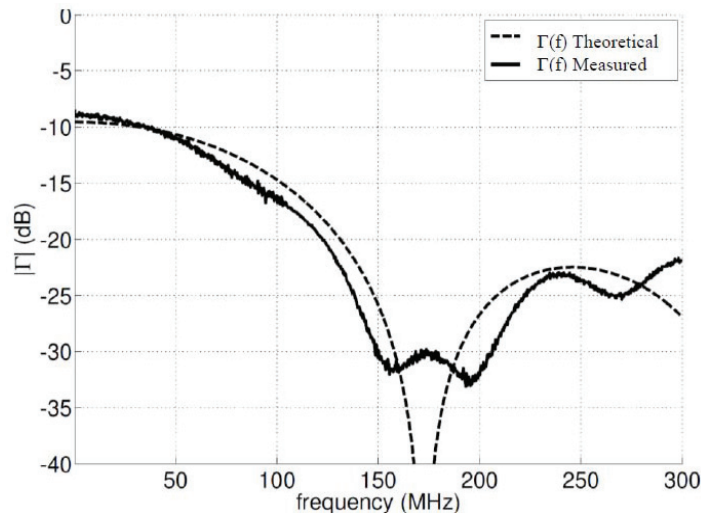


Fig 20. Measured and calculated magnitude of the reflection coefficient. Notice the coincidence of the resonance frequency. Both responses are in acceptable agreement.

VIII. FREQUENCY DOMAIN MEASUREMENTS

The tapered transmission line adaptor was also characterized in the frequency domain. A Vector Network Analyzer (VNA) Anritsu MS4630A was connected to Port 1. Port 2 was terminated using a coaxial 100 Ω load. The measurements were performed over a frequency band from 10 kHz to 300 MHz

The results of the measurement and the analytical calculation of $\Gamma(f)$ are presented in Fig 20. It can be seen that the theoretical results are in good agreement with experimental data and the minimum matching frequency is below 50 MHz. The first resonant frequency is about 170 MHz

As the frequency domain measurements shows, the adaptor works better at high frequencies. However, at frequencies lower than the 50 MHz limit, the reflection coefficient remains nearly equal to the required -10 dB matching threshold. In fact, near DC the transmission line is much shorter than the wavelength and the impedance that is seen at Port 1 is directly the impedance of Port 2, the reflection coefficient of which is

$$\Gamma(DC) = \frac{Z_L - Z_o}{Z_L + Z_o} = -9.54 \text{ (dB)} \quad (27)$$

This fact and the calculated transfer function showed in Fig 10 explain why the tapered adaptor can transport pulsesignals, preserving the rise time (high frequency content) without attenuating significantly the decaying part of the pulse (low frequency content).

IX. CONCLUSIONS

We described the simulation, design, realization and experimental test of a tapered transmission line for adapting a broadband impulse generator to a radiating antenna, for a frequency range of 50 MHz to 1 GHz. Two different taper geometries were considered and discussed in the analysis: exponential and logarithmic. Two analysis methods were also used: (1) analytical equations obtained by applying the transmission line theory, and (2) numerical simulations in both frequency- and time-domain using Comsol®.

It was shown that in general an exponential taper performs better than a logarithmic one, especially at high frequencies. Time domain simulations revealed that for fast transient subnanosecond pulses, both tapers can be used equivalently and the signal does not suffer from any significant distortion while traveling along the tapers.

We also showed that analytical equations obtained using the transmission line theory are in very good agreement with full-wave simulation results and can be used advantageously in the design of tapers.

We finally presented the mechanical design and the realization of an exponential taper used for the connection of a 50- Ω pulser to a Half Impulse Radiating Antenna (HIRA) having an input impedance $Z_A = 100 \Omega$. Such a radiating system can be used in EMC testing of devices subject to intentional electromagnetic interferences. The realized taper was fully characterized in frequency-domain using a vector analyzer and in time domain using a reflectometer and shown to be performing in agreement with the simulations.

X. ACKNOWLEDGMENTS

This work is financially supported by the EPFL-SDC (Swiss Agency for Development and Cooperation) Fund and the Cattleya project.

XI. REFERENCES

- [1] C. R. Paul, *Introduction to EMC*: Wiley, 2006.
- [2] L. N. Dworsky, *Modern transmission line theory and applications / Lawrence N. Dworsky*. New York :: Wiley, 1979.
- [3] C. E. Baum and J. M. Lehr, "Tapered transmission-line transformers for fast high-voltage transients," *Plasma Science, IEEE Transactions on*, vol. 30, pp. 1712-1721, 2002.
- [4] E. G. Farr and G. D. Sower, "Design Principles of Half-Radiating Antennas," *Sensor and Simulation 0390*, 1995.
- [5] C. E. Baum, "Radiation of Impulse-Like Transient Fields," *Sensor and Simulation 0321*, Nov 1989.
- [6] D. V. Giri, *High-power electromagnetic radiators: nonlethal weapons and other applications* Harvard University Press, 2004.
- [7] R. E. Collin, "The Optimum Tapered Transmission Line Matching Section," *Proceedings of the IRE*, vol. 44, pp. 539-548, April 1956.
- [8] R. W. Klopfenstein, "A Transmission Line Taper of Improved Design," *Proceedings of the IRE*, vol. 44, pp. 31-35, 1956.
- [9] C. W. Hsue, "Time-domain scattering parameters of an exponential transmission line," *Microwave Theory and Techniques, IEEE Transactions on*, vol. 39, pp. 1891-1895, November 1991.
- [10] M. C. R. Carvalho and W. Margulis, "Laser diode pumping with a transmission line transformer," *Microwave and Guided Wave Letters, IEEE*, vol. 1, pp. 368-370, 1991.

- [11] C. W. Hsue and C. D. Hechtman, "Transient responses of an exponential transmission line and its applications to high-speed backdriving in in-circuit test," *Microwave Theory and Techniques, IEEE Transactions on*, vol. 42, pp. 458-462, 1994.
- [12] M. C. R. Carvalho, *et al.*, "A new, small-sized transmission line impedance transformer, with applications in high-speed optoelectronics," *Microwave and Guided Wave Letters, IEEE*, vol. 2, pp. 428-430, 1992.
- [13] M. G. Case, "Nonlinear Transmission Lines for Picosecond Pulse, Impulse and Millimeter-Wave Harmonic Generation," Ph. D Thesis, Electrical and Computer Engineering, University of California Santa Barbara, Santa Barbara, 1993.
- [14] G. M. Yang, *et al.*, "Ultrawideband (UWB) Antennas With Multiresonant Split-Ring Loops," *Antennas and Propagation, IEEE Transactions on*, vol. 57, pp. 256-260, 2009.
- [15] D. V. Giri, "Swiss Half IRA (SWIRA) Design Considerations," in *Workshop on electromagnetic effects to infrastructure*, Spiez, Switzerland, 2005.
- [16] D. M. Pozar, *Microwave Engineering*: Wiley, 1997.